

# Fully conservative hydraulic jumps and solibores in two-layer Boussinesq fluids

Jānis Priede

Fluid and Complex Systems Research Centre, Coventry University,  
Coventry, CV1 5FB, United Kingdom

## Abstract

We consider a special type of hydraulic jumps (internal bores) which, in the vertically bounded system of two immiscible fluids with slightly different densities, conserve not only the mass and impulse but also the circulation and energy. This is possible only at specific combinations of the upstream and downstream states. Two such combinations are identified with arbitrary upstream and downstream interface heights. The first has a cross symmetry between the interface height and shear on both sides of the jump. This symmetry, which is due to the invariance of the two-layer shallow-water system with swapping the interface height and shear, ensures the automatic conservation of the impulse and energy as well as the continuity of characteristic velocities across the jump. The speed at which such jumps propagate is uniquely defined by the conservation of the mass and circulation. The other possibility is a marginally stable shear flow which can have fully conservative jumps with discontinuous characteristic velocities. Both types of conservative jumps are shown to represent a long-wave approximation to the so-called solibores which appear as smooth permanent-shape solutions with the same properties in a weakly non-hydrostatic model. A new analytical solution for solibores is obtained and found to agree very well with the previous DNS results for partial-depth lock release flow. The finding that certain large-amplitude hydraulic jumps can be fully conservative, while most are not such even in the inviscid approximation, points toward the wave dispersion as a primary mechanism behind the lossy nature of internal bores.

## 1 Introduction

Hydraulic jumps are steep variations in the height of the liquid surface which can propagate at a nearly constant speed over relatively large distances. Such step-like gravity waves are often referred to as bores. A well-known example is that of tidal bores (Simpson, 1999). Hydraulic jumps can form also in stably stratified fluids where they are known as internal bores (Baines, 1995). The latter occur in various geophysical flows, such as coastal oceans (Scotti & Pineda, 2004) and the inversion layers in the atmosphere (Christie & White, 1992).

One of the key characteristics of hydraulic jumps is their speed of propagation. Determination of this speed theoretically is difficult because the flow associated with bores tends

to be very complex and often turbulent. Notwithstanding this complexity, the speed at which a bore propagates can be determined approximately by considering the conservation of relevant quantities. In single fluid layers, the speed of propagation is determined by the conservation of the mass and momentum fluxes across the front of the bore. Application of the respective conservation laws integrally to a box enclosing the jump constitutes the basis of the hydraulic approximation, also known as the control volume method (Rayleigh, 1914).

The same front speed is defined also by the Rankine-Hugoniot jump conditions for the hydrostatic shallow-water (SW) equations governing the conservation of mass and momentum in single fluid layers (Whitham, 1974). The momentum, however, is not the only dynamical quantity that can be conserved. The hydrostatic SW equations admit an infinite number of locally conserved quantities (Whitham, 1974, p. 459). But only one such quantity can in general be conserved besides the mass. For example, the jumps conserving momentum do not in general conserve energy. The preference for momentum over energy as a conserved quantity is motivated by physical considerations. Namely, the loss of energy can be attributed to the viscous dissipation in strongly turbulent bores. Turbulence can also generate vorticity by stretching and tilting vortices which breaks the conservation of the vorticity flux across the jump. However, there is no analogous physical mechanism by which turbulence or viscosity could affect the flux of momentum across the jump.

The same considerations apply also to two-layer systems. However, there are a few significant differences which concern two-layer systems bounded by a rigid lid. The principal difference is a longitudinal pressure gradient. It appears in this case due to the fixed total height and ensures that the volumetric flux in one layer is equal but opposite to that in the other layer. This makes the basic SW equations for separate layers non-local. As a result, the longitudinal momentum is not in general conserved in such systems (Camassa *et al.*, 2012). But it does not mean that the two-layer hydrostatic SW equations are inherently non-local as it is often thought (Fyhn *et al.*, 2019). These equations can be represented in a number of locally conservative forms which are mathematically equivalent as long as the waves are smooth (Priede, 2022). Firstly, there is a circulation conservation equation (Sandstrom & Quon, 1993). It yields the same speed of propagation as the vorticity front condition obtained by Borden & Meiburg (2013) using the conventional control-volume approach. Secondly, there is also a momentum-like quantity, called pseudo-momentum or impulse (Benjamin, 1986), which is conserved locally in two-layer systems bounded by a rigid lid. However, in contrast to the single-layer case, the respective two-layer SW conservation equation is not uniquely defined. It contains a free parameter  $\alpha$  defining the relative contribution of each layer to the pressure at the interface (Priede, 2022). This parameter affects only the hydraulic jumps but not continuous waves. The Rankine-Hugoniot jump conditions resulting from the mass and impulse conservation equations with  $\alpha = 1$  and  $\alpha = -1$  are mathematically equivalent to the classical front conditions for internal bores obtained by Wood & Simpson (1984) and Klemp *et al.* (1997), respectively. The latter also includes the front condition of Benjamin (1968) for gravity currents. The vorticity front condition of Borden & Meiburg (2013) is in turn recovered in the limit  $|\alpha| \rightarrow \infty$ .

Since the speed of propagation predicted by the SW model depends on  $\alpha$ , circulation like energy is not in general conserved by the jumps that conserve the mass and impulse. There are, however, a few exceptions that correspond to the jumps whose speed of propagation does not depend on  $\alpha$ . Such jumps, which conserve all four quantities, are the focus of the

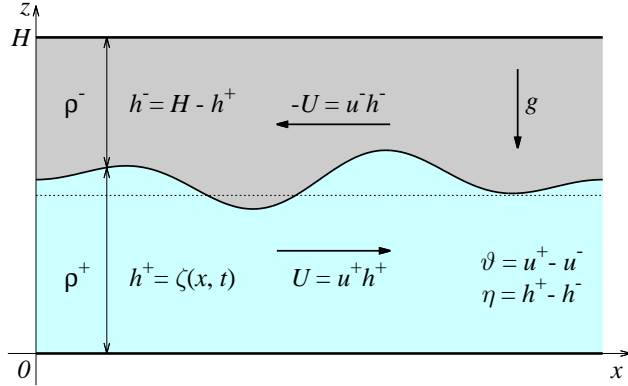


Figure 1: Sketch of the problem showing a horizontal channel of a constant height  $H$  bounded by two parallel solid walls and filled with two inviscid immiscible fluids with constant densities  $\rho^+$  and  $\rho^-$ , where  $h^+ = \zeta(x, t)$  and  $h^- = H - h^+$  are the depths of the bottom and top layers, respectively.

present paper. We show that these fully conservative jumps represent a long-wave approximation to the solibores which are permanent-shape smooth solutions appearing in the weakly non-hydrostatic approximation (Esler & Pearce, 2011). We also obtain an exact analytical solution for such solibores and find a good fit with the numerical results of Khodkar *et al.* (2017) for the partial-height lock-exchange flow in a two-layer system with a small density contrast.

The paper is organized as follows. In section 2, we formulate the problem and present the basic equations including the generalized SW momentum equation. Jump conditions are introduced and analysed in section 3. In section 4, we show that the characteristics of fully conservative jumps are the same as those of solibores and obtain a relatively simple analytical solution for the latter. The paper is concluded with section 5 which contains a summary and discussion of the main results including a comparison with numerical results.

## 2 Two-layer SW model

Consider a horizontal channel of a constant height  $H$  which is bounded by two parallel solid walls and filled with two inviscid immiscible fluids with constant densities  $\rho^+$  and  $\rho^-$  as shown in Fig. 1. The fluids are subject to a downward gravity force with the free fall acceleration  $g$ . The interface separating the fluids is located at the height  $z = \zeta(x, t)$ , which is equal to the depth of the bottom layer  $h^+$  and varies with the horizontal position  $x$  and the time  $t$ . The velocity  $\mathbf{u}^\pm$  and the pressure  $p^\pm$  in each layer are governed by the Euler equation

$$\partial_t \mathbf{u} + \mathbf{u} \cdot \nabla \mathbf{u} = -\rho^{-1} \nabla p + \mathbf{g} \quad (1)$$

and the incompressibility constraint  $\nabla \cdot \mathbf{u} = 0$ . Henceforth, for the sake of brevity, we drop  $\pm$  indices wherever analogous expressions apply to both layers. At the interface  $z = \zeta(x, t)$ ,

we have the continuity of pressure,  $[p] \equiv p^+ - p^- = 0$ , and the kinematic condition

$$w = \frac{d\zeta}{dt} = \zeta_t + u\zeta_x, \quad (2)$$

where  $u$  and  $w$  are the  $x$  and  $z$  components of velocity, and the subscripts  $t$  and  $x$  stand for the corresponding partial derivatives.

To make the paper self-contained, below we shall present a brief derivation of the basic shallow water equations. Firstly, integrating the incompressibility constraint over the depth of each layer and using (2), we obtain

$$h_t + (h\bar{u})_x = 0, \quad (3)$$

where the overbar denotes the depth average. Secondly, doing the same for the horizontal ( $x$ ) component of (1), we have

$$(h\bar{u})_t + (h\bar{u^2})_x = -\rho^{-1}h\bar{p}_x. \quad (4)$$

Pressure is obtained by integrating the vertical ( $z$ ) component of (1) as follows

$$p(x, z, t) = \Pi(x, t) + \rho \int_{\zeta}^z (w_t + \mathbf{u} \cdot \nabla w - g) dz, \quad (5)$$

where  $\Pi(x, t) = p^{\pm}(x, z, t)|_{z=\zeta}$  is the distribution of pressure along the interface. Thirdly, averaging the  $x$ -component of the gradient of the pressure (5) over the depth of each layer, after a few rearrangements, we obtain

$$\bar{p}_x = \left( \Pi + \rho g \zeta + \rho \overline{(z - z_0)(w_t + \mathbf{u} \cdot \nabla w)} \right)_x, \quad (6)$$

which defines the RHS of (4) with  $z_0 = 0$  and  $z_0 = H$  for the bottom and top layers, respectively.

When the characteristic horizontal length scale  $L$  is much larger than the height  $H$  :  $H/L = \epsilon \ll 1$ , the exact depth-averaged equations obtained above can be simplified using the shallow-water approximation. In this case, the incompressibility constraint implies  $w/u = O(\epsilon)$  and (6) correspondingly reduces to

$$\bar{p}_x = (\Pi + \rho g \zeta)_x + O(\epsilon^2), \quad (7)$$

where the leading-order term is purely hydrostatic and  $O(\epsilon^2)$  represents a small dynamical pressure correction due to the vertical velocity  $w$ . Besides that the flow in both layers is considered to be irrotational:  $\boldsymbol{\omega} = \nabla \times \mathbf{u} = 0$ . According to the inviscid vorticity equation  $\frac{d\boldsymbol{\omega}}{dt} = (\boldsymbol{\omega} \cdot \nabla) \mathbf{u}$ , this property is preserved by (1). In the leading-order approximation, the irrotationality constraint reduces to  $\partial_z u^{(0)} = 0$ . It means that the horizontal velocity can be written as

$$u = \bar{u} + \tilde{u}, \quad (8)$$

where the deviation from the average  $\bar{u}$  implied by (7) is  $\tilde{u} = O(\epsilon^2)$ . Consequently, in the second term of (4), we can substitute  $\overline{u^2} = \bar{u}^2 + O(\epsilon^4)$ . Finally, using (3) and ignoring the  $O(\epsilon^2)$  dynamic pressure correction, (4) can be written as

$$\rho \left( \bar{u}_t + \frac{1}{2} \bar{u}^2 + g\zeta_x \right) = -\Pi_x. \quad (9)$$

This equation along with (3) constitute the basic set of SW equations in the leading-order (hydrostatic) approximation.

The vertical velocity, which gives rise to a non-hydrostatic pressure perturbation, follows from the incompressibility constraint and (8) as

$$w(z) = - \int_{z_0}^z u_x dz = -(z - z_0) \bar{u}_x + O(\epsilon^2), \quad (10)$$

where  $z_0$  is defined as in (6) to satisfy the impermeability conditions  $w(0) = w(H) = 0$ . Substituting this into (6), after a few transformations, we obtain the well-known result (Green & Naghdi, 1976; Liska *et al.*, 1995; Choi & Camassa, 1999)

$$h \bar{p}_x^{(1)} = -\frac{1}{3} \rho (h^3 (D_t \bar{u}_x - \bar{u}_x^2)_x + O(\epsilon^4)) = \frac{1}{3} \rho (h^2 D_t^2 h)_x + O(\epsilon^4), \quad (11)$$

where  $D_t \equiv \partial_t + \bar{u} \partial_x$  and  $\bar{u}_x = -h^{-1} D_t h$ . The latter relation follows from (3) and ensures that (2) is satisfied by (10) up to  $O(\epsilon^2)$ .

The system of four SW equations (9) and (3) contains five unknowns:  $u^\pm$ ,  $h^\pm$  and  $\Pi$ , and is completed by adding the fixed height constraint  $\{h\} \equiv h^+ + h^- = H$ . Henceforth, we simplify the notation by omitting the bar over  $u$  and using the curly brackets to denote the sum of the enclosed quantities.

Two more unknowns are eliminated as follows. Firstly, adding the mass conservation equations for each layer together and using  $\{h\}_t \equiv 0$ , we obtain  $\{u h\} = \Phi(t)$ , which is the total flow rate. The channel is assumed to be laterally closed, which means  $\Phi \equiv 0$ , and, thus,  $u^- h^- = -u^+ h^+$ . Secondly, the pressure gradient  $\Pi_x$  can be eliminated by subtracting the two equations (9) one from another. This leaves only two unknowns,  $U \equiv u^+ h^+$  and  $h = h^+$ , and two equations, which can be written in a locally conservative form as

$$(\{\rho/h\} U)_t + \left( \frac{1}{2} [\rho/h^2] U^2 + g [\rho] h \right)_x = - [\bar{p}_x^{(1)}], \quad (12)$$

$$h_t + U_x = 0. \quad (13)$$

where the square brackets denote the difference of the enclosed quantities between the bottom and top layers:  $[f] \equiv f^+ - f^-$ . The pressure correction on the RHS of (12), which is defined by (11), can be cast in the following locally conservative form

$$\bar{p}_x^{(1)} = \frac{\rho}{3} \left( (h D_t^2 h + \frac{1}{2} (D_t h)^2 - h_t D_t h)_x + (h_x D_t h)_t \right). \quad (14)$$

In the hydrostatic approximation, which will be considered first, this dynamical pressure correction is irrelevant.

In the following, the density difference is assumed to be small. According to the Boussinesq approximation, this difference is important only for the gravity of fluids, which drives the flow. For the inertia, this difference is ignored, which simplifies the problem significantly. A further simplification is achieved by using the total height  $H$  and the characteristic gravity wave speed  $C = \sqrt{2Hg[\rho]/\{\rho\}}$  as the length and velocity scales, respectively, and  $H/C$  as the time scale.

In the hydrostatic Boussinesq approximation, (12) and (13) take a remarkably symmetric form (Milewski & Tabak, 2015):

$$\vartheta_t + \frac{1}{2} (\eta(1 - \vartheta^2))_x = 0, \quad (15)$$

$$\eta_t + \frac{1}{2} (\vartheta(1 - \eta^2))_x = 0, \quad (16)$$

where  $\eta = [h]$  and  $\vartheta = [u]$  are the dimensionless depth and velocity differentials between the top and bottom layers. Subsequently, the former is referred to as the interface height and the latter as the shear velocity. Note that this basic system of two-layer SW equations is invariant to swapping  $\eta$  and  $\vartheta$ . The same symmetry holds also for the momentum and energy equations

$$(\eta\vartheta)_t + \frac{1}{4}(\eta^2 + \vartheta^2 - 3\eta^2\vartheta^2)_x = 0, \quad (17)$$

$$(\eta^2 + \vartheta^2 - \eta^2\vartheta^2)_t + (\eta\vartheta(1 - \eta^2)(1 - \vartheta^2))_x = 0, \quad (18)$$

which are obtained by multiplying (15) with  $\eta$  and  $\eta^2\vartheta$ , respectively, and then using (16) to convert the resulting expression into locally conservative form. It is important to note that this  $\eta \leftrightarrow \vartheta$  symmetry is limited to the Boussinesq approximation. Also, note that the conserved quantity  $\eta\vartheta$  in (17) represents a pseudo-momentum (impulse) (Priede, 2022). An infinite sequence of further conservation laws can be constructed in a similar way (Milewski & Tabak, 2015). The generalized momentum equation can formally be obtained by multiplying (15) with an arbitrary constant  $\alpha$  and adding to (17):

$$((\eta + \alpha)\vartheta)_t + \frac{1}{4}(\eta^2 + \vartheta^2 - 3\eta^2\vartheta^2 + 2\alpha\eta(1 - \vartheta^2))_x = 0. \quad (19)$$

For a more detailed derivation of equations (17)–(19), we refer to Priede (2022).

The constant  $\alpha$  in (19), which defines the relative contribution of each layer to the pressure gradient along the interface, is supposed to depend only on the ratio of densities. For nearly equal densities, which is the case covered by the Boussinesq approximation,  $\alpha \approx 0$  can be expected. This corresponds to both layers affecting the pressure at the interface with equal weight coefficients. Note that with  $\alpha = 0$  (19) reduces to the basic momentum equation (17) so restoring the  $\eta \leftrightarrow \vartheta$  symmetry of the Boussinesq approximation. This symmetry is recovered also in the limit  $|\alpha| \rightarrow \infty$ , in which (19) reduces to the circulation conservation equation (15).

Two-layer SW equations for Boussinesq fluids can also be written in the canonical form

$$R_t^\pm - \lambda^\pm R_x^\pm = 0, \quad (20)$$

where

$$R^\pm = -\eta\vartheta \pm \sqrt{(1 - \eta^2)(1 - \vartheta^2)} \quad (21)$$

are the Riemann invariants and

$$\lambda^\pm = \frac{3}{4}R^\pm + \frac{1}{4}R^\mp = -\eta\vartheta \pm \frac{1}{2}\sqrt{(1 - \eta^2)(1 - \vartheta^2)} \quad (22)$$

are the associated characteristic velocities (Long, 1956; Cavanie, 1969; Ovsyannikov, 1979; Sandstrom & Quon, 1993; Baines, 1995; Chumakova *et al.*, 2009).

For the interface confined between the top and bottom boundaries, which corresponds to  $\eta^2 \leq 1$ , the characteristic velocities (22) are real and, thus, the equations are of hyperbolic type if  $\vartheta^2 \leq 1$ . The latter constraint on the shear velocity ensures the absence of the long-wave Kelvin-Helmholtz instability which would otherwise disrupt the interface (Milewski *et al.*, 2004). It has to be noted that this instability is different from the usual short-wave Kelvin-Helmholtz which does not appear in the hydrostatic SW approximation (Esler & Pearce, 2011).

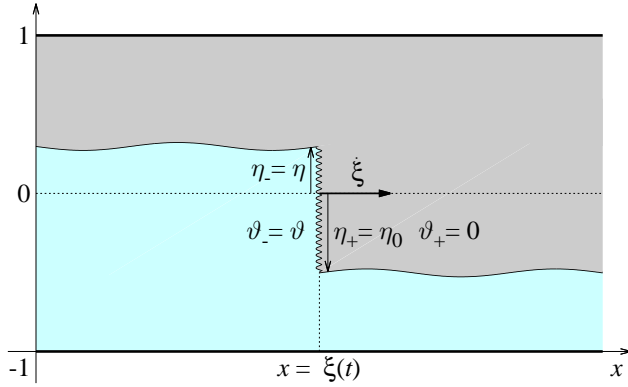


Figure 2: A jump with the upstream interface height  $\eta_- = \eta$  and the shear velocity  $\vartheta_- = \vartheta$  propagating at the speed  $\dot{\xi}$  into a still fluid ahead ( $\vartheta_+ = 0$ ) with the interface located at the height  $\eta_+ = \eta_0$ .

### 3 Hydraulic jumps

Consider a discontinuity in  $\eta$  and  $\vartheta$  at the point  $x = \xi(t)$  across which the respective variables jump by  $[\![\eta]\!] \equiv \eta_+ - \eta_-$  and  $[\![\vartheta]\!] \equiv \vartheta_+ - \vartheta_-$ . Here the plus and minus subscripts denote the corresponding quantities at the front and behind the jump. The double-square brackets stand for the differential of the enclosed quantity across the jump. Integrating (16) and (19) across the jump, which is equivalent to substituting the spatial derivative  $f_x$  with  $[\![f]\!]$  and the time derivative  $f_t$  with  $-\dot{\xi} [\![f]\!]$  (Whitham, 1974), the jump propagation velocity can be expressed, respectively, as (Priede, 2022)

$$\dot{\xi} = \frac{1}{2} \frac{[\![\vartheta(1 - \eta^2)]\!]}{[\![\eta]\!]}, \quad (23)$$

$$\dot{\xi} = \frac{1}{4} \frac{[\![\eta^2 + \vartheta^2 - 3\eta^2\vartheta^2 + 2\alpha(1 - \vartheta^2)]\!]}{[\!(\eta + \alpha)\vartheta]\!}. \quad (24)$$

For a jump to be feasible, it has to satisfy the hyperbolicity constraint  $\vartheta_\pm^2 \leq 1$  as well as the energy constraint. The latter follows from the integration of (18) across the jump and defines the associated energy production rate (Priede, 2022)

$$\dot{\varepsilon} = [\![\eta\vartheta(1 - \eta^2)(1 - \vartheta^2)]\!] - \dot{\xi} [\![\eta^2 + \vartheta^2 - \eta^2\vartheta^2]\!] \leq 0, \quad (25)$$

which cannot be positive as the energy can only be dissipated or dispersed but not generated by the jump.

Applying (23) and (24) to a jump with the upstream interface height  $\eta_- = \eta$  propagating into a quiescent fluid ( $\vartheta_+ = 0$ ) with the interface located at the height  $\eta_+ = \eta_0$ , as shown in Fig. 2, after a few rearrangements, we obtain:

$$\vartheta_-^\pm = \pm \frac{(\eta_0 - \eta)(\eta_0 + \eta + 2\alpha)^{1/2}}{((1 - \eta^2)(\eta_0 - \eta) + 2(\eta + \alpha)(1 - \eta_0\eta))^{1/2}}, \quad (26)$$

$$\dot{\xi}^\pm = -\vartheta_-^\pm \frac{1 - \eta^2}{2(\eta_0 - \eta)}, \quad (27)$$

where  $\vartheta_-^\pm$  is the upstream shear velocity and the plus and minus signs refer to the opposite directions of propagation, i.e.,  $\dot{\xi}^+ = -\dot{\xi}^-$ , which are both permitted by the mass and momentum balance conditions. Because the energy balance (25) changes sign with the direction of propagation, only one direction of propagation is in general permitted for each jump. This does not apply to the jumps which satisfy (25) exactly. Such energy-conserving jumps, which can in principle propagate downstream as well as upstream, will be considered in the following.

A distinctive feature of these jumps is the invariance of their velocity of propagation (27) with  $\alpha$  (Priede, 2022). It implies that these jumps conserve also circulation. If this is the case, the  $\alpha$  terms in the generalized momentum equation (19) cancel out so making the associated jump condition independent of  $\alpha$ . For this to happen, the shear velocity (26) at  $\alpha = 0$  has to be the same as that at  $\alpha \rightarrow \infty$ . This requirement results in  $\eta(\eta - \eta_0) = 0$ , which has two solutions:  $\eta = \eta_0$  and  $\eta = 0$ . The first one is irrelevant as it corresponds to a uniform state with a constant interface height  $\eta_0$ . The second one describes a jump from  $\eta_0$  to the layer mid-height  $\eta = 0$ . The corresponding upstream shear velocity and the speed of propagation following from (26) and (27) are  $\vartheta_-^\pm = \pm\eta_0$  and  $\dot{\xi}^\pm = \mp\frac{1}{2}$ .

Owing to the symmetry of this jump  $\vartheta_\pm = \eta_\mp$ , the impulse and energy are conserved automatically, i.e., independently of the velocity of propagation. Besides that the same symmetry makes both characteristic velocities (22) continuous across the jump:  $[\![\lambda^\pm]\!] = 0$ . It means that the positive, as well as negative characteristics, emanating upstream from the jump are parallel to the corresponding characteristics emanating downstream. Likewise continuous are also the Riemann invariants (21).

The above properties are shared by a broader class of fully conservative jumps which can be sustained by a non-zero downstream shear ( $\vartheta_+ \neq 0$ ). The continuity condition  $[\![\lambda^\pm]\!] = 0$ , which after a few rearrangements can be rewritten as  $[\!(\eta \pm \vartheta)\!] = 0$ , yields two pairs of possible solutions:

$$(\eta_+, \vartheta_+) = \pm(\eta_-, \vartheta_-), \quad (28)$$

$$(\eta_+, \vartheta_+) = \pm(\vartheta_-, \eta_-). \quad (29)$$

The first solution corresponding to the plus sign in (28) is continuous and so irrelevant. The other three are symmetric jumps which automatically satisfy the energy balance condition (25) as well as that of the impulse (24) with  $\alpha = 0$ . The second solution corresponding to the minus sign in (28), which represents a centrally symmetric jump, conserves the mass and circulation only if  $\vartheta_+ = \pm\eta_+$  and  $\dot{\xi} = \pm\frac{1}{2}(1 - \eta_+^2)$ . This is just a particular case of a more general solution that follows from the mass and circulation conservation laws for the second pair of jumps (29). In this case, we obtain the speed of propagation which can be written in terms of the upstream and downstream interface heights as

$$\dot{\xi}^\pm = \pm\frac{1}{2}(1 + \eta_+\eta_-). \quad (30)$$

The corresponding shear velocities according to (29) are  $(\vartheta_+, \vartheta_-) = \mp(\eta_-, \eta_+)$ . Note that the previous two solutions with  $\eta_+ = 0$  and  $\eta_+ = -\eta_-$  are particular cases of (30).

In marginally hyperbolic shear flows with  $\vartheta_+ = \vartheta_- = \mp 1$ , which is a very specific case, fully conservative jumps with discontinuous characteristic velocities are possible. Such jumps propagate at the speed  $\dot{\xi}^\pm = \pm \frac{1}{2}(\eta_+ + \eta_-)$  which ensures the conservation of impulse and mass, whilst the energy and circulation are conserved automatically.

In the next section, we show that these fully conservative hydraulic jumps represent a long-wave approximation to the so-called solibores which appear as permanent-shape solutions in the weakly non-hydrostatic approximation described by (11) (Esler & Pearce, 2011).

## 4 Weakly non-hydrostatic analytical solution for solibores

Let us now turn to a weakly non-hydrostatic approximation, which is defined by the dynamical pressure correction (14) in the circulation conservation equation (12), and search for permanent-shape waves travelling at the speed  $c$ . Such waves are stationary in the co-moving frame of reference where they vary depending only on  $x' = x - ct$ . With the time derivative written as  $\partial_t \equiv -c\partial_x$ , the last two terms in (14) cancel out, and correspondingly (12) and (13) take the form

$$\left(\frac{1}{2}\eta(1 - \vartheta^2) - c\vartheta\right)_x = -\frac{1}{3} [hD_t^2h + \frac{1}{2}(D_t h)^2]_x, \quad (31)$$

$$\left(\frac{1}{2}\vartheta(1 - \eta^2) - c\eta\right)_x = 0, \quad (32)$$

where  $h$  stands for  $h^\pm = \frac{1}{2}(1 \pm \eta)$  and  $D_t$  for  $D_t^\pm \equiv (u^\pm - c)\partial_x$  with the plus and minus indices referring to the top and bottom layers. Now (31) and (32) can be integrated once to obtain

$$\frac{1}{2}\eta(1 - \vartheta^2) - c(\vartheta - \vartheta_0) = -\frac{1}{3} [hD_t^2h + \frac{1}{2}(D_t h)^2], \quad (33)$$

$$\frac{1}{2}\vartheta(1 - \eta^2) - c(\eta - \eta_0) = 0, \quad (34)$$

where  $\vartheta_0$  and  $\eta_0$  are the constants of integration. Note that if the fluid is quiescent ( $\vartheta = 0$ ), then according to (34)  $\eta_0$  is equal to the interface height;  $c\vartheta_0 = A$  is the flux of circulation which is one of the conserved quantities.

Using the identity  $hD_t^\pm \equiv -h_0^\pm c\partial_x$ , which follows from  $D_t^\pm \equiv (u^\pm - c)\partial_x$  and (34) when written in terms of the original variables as  $h^\pm(u^\pm - c) = -h_0^\pm c$ , the RHS of (33) can be transformed as follows

$$-\frac{c^2}{3} [h_0^2 ((h_x/h)_x + \frac{1}{2} (h_x/h)^2)] = -\frac{c^2}{3} \{(h_0 h_x)^2/h\}_x / \eta_x.$$

Then multiplying (33) with  $\eta_x$  and using (32) to substitute  $c\eta_x$ , after a few rearrangements, the resulting equation can be integrated once more to obtain

$$A\eta + B - \frac{1}{4}(1 - \eta^2)(1 + \vartheta^2) = -\frac{c^2}{12} \frac{1 - 2\eta_0\eta + \eta_0^2}{1 - \eta^2} \eta_x^2,$$

where  $B$  is a constant of integration which represents another conserved quantity, the flux of impulse. Finally, using (34) to eliminate  $\vartheta$ , we obtain

$$\eta_x^2 + P(\eta) = 0, \quad (35)$$

where

$$P(\eta) = -\frac{3}{c^2} \frac{(1-\eta^2)(1-\eta^2-4(A\eta+B)) + 4c^2(\eta-\eta_0)^2}{1-\eta^2+(\eta-\eta_0)^2} \quad (36)$$

is analogous to potential energy when  $\eta_x^2$  is interpreted as kinetic energy with  $x$  representing the time. Thus (35) can be thought of as describing the conservation of total energy for a body performing oscillations in the potential well defined by (36). The oscillations occur between two extremes of  $\eta$  at which  $\eta_x = 0$ . According to (35) these points are the zeros of the numerator of  $P(\eta)$ . As the latter is a quartic function of  $\eta$ , it can have in general four roots. For a finite-amplitude solution to be possible, all roots have to be real (Esler & Pearce, 2011). If two roots coincide but the other two are distinct, the oscillation period becomes infinite resulting in the so-called solitary wave. If also the other two roots coincide so that there are two distinct double roots, we end up with only a half-solitary wave which is termed the solibore (Esler & Pearce, 2011).

In the following, we focus on the last case and determine the unknown constants in (36) by factorizing the numerator of  $P(\eta)$  as follows

$$(1-\eta^2)(1-\eta^2-4(A\eta+B)) + 4c^2(\eta-\eta_0)^2 = (\eta-\eta_+)^2(\eta-\eta_-)^2, \quad (37)$$

where  $\eta_+$  and  $\eta_-$  are two double roots of the quartic defining respectively the upstream and downstream interface heights. Comparing the coefficients at the same powers of  $\eta$  on both sides of (37) and eliminating  $A$  and  $B$ , we have

$$4c^2(1 \pm \eta_0)^2 = (\eta_+ + \eta_- \pm (1 + \eta_+\eta_-))^2, \quad (38)$$

which represents a system of two equations corresponding to the same choice of sign on both sides. There are two solutions for  $c$  and  $\eta_0$  possible depending on the combination of signs when taking the square root of both sides of (38). The first solution

$$c = \pm \frac{1}{2}(1 + \eta_+\eta_-), \quad \eta_0 = \frac{\eta_+ + \eta_-}{1 + \eta_+\eta_-},$$

with  $(\vartheta_+, \vartheta_-) = \mp(\eta_-, \eta_+)$  following from (34) corresponds to the conservative jumps with continuous characteristic velocities found in the previous section. The second solution

$$c = \pm \frac{1}{2}(\eta_+ + \eta_-), \quad \eta_0 = \frac{1 + \eta_+\eta_-}{\eta_+ + \eta_-},$$

with  $\vartheta_+ = \vartheta_- = \mp 1$  resulting from (34) corresponds to the conservative jumps with discontinuous characteristic velocities. This type of solibores seems to be of little practical relevance because of the very specific shear value required for their existence.

Using the factorization of the numerator of  $P(\eta)$  defined by (37), we can integrate (35) analytically as follows

$$\begin{aligned} x(\eta) &= \frac{c}{\sqrt{3}} \int \frac{q(\eta) d\eta}{(\eta-\eta_+)(\eta-\eta_-)} \\ &= \frac{2c}{\sqrt{3}(\eta_+ - \eta_-)} \left[ q(\eta_+) \operatorname{arctanh} \left( \frac{q(\eta)}{q(\eta_+)} \right) - q(\eta_-) \operatorname{arctanh} \left( \frac{q(\eta_-)}{q(\eta)} \right) \right], \end{aligned} \quad (39)$$

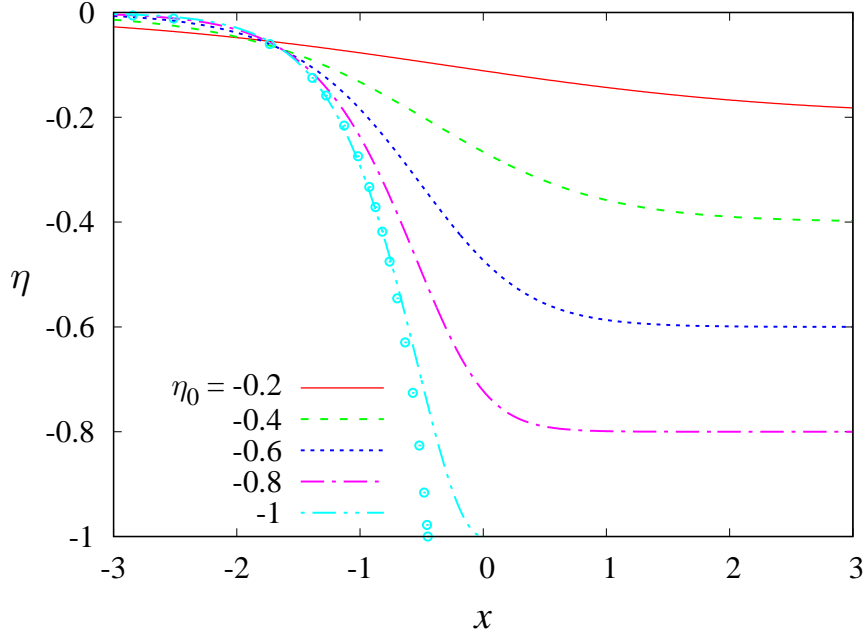


Figure 3: Solibores advancing into a quiescent downstream state with various interface heights  $\eta_0 < 0$ . The dots show the approximate solution of Benjamin (1968) for energy-conserving gravity current.

where  $q(\eta) = \sqrt{1 - \eta^2 + (\eta - \eta_0)^2}$  and  $\eta_+$  and  $\eta_-$  are ordered so that  $q(\eta_+) \geq q(\eta_-)$ . In the symmetric continuous case  $\eta_+ = -\eta_-$ , when  $\eta_0 = 0$  and  $c = \pm(1 - \eta_+^2)/2$ , (39) can be written explicitly as  $\eta(x) = \eta_+ \tanh\left(\frac{2\sqrt{3}x}{\eta_+ - \eta_-}\right)$ .

For a quiescent downstream state, when  $\vartheta_+ = \eta_- = 0$ ,  $\eta_0 = \eta_+$  and  $c = \pm\frac{1}{2}$ , which is practically the most relevant, (39) is plotted in Fig. 3a for various interface heights  $\eta_0 < 0$ . Note that (39) is invariant with the symmetry transformation  $\eta \rightarrow -\eta$ . Therefore, the solutions with  $\eta_0 > 0$  are mirror symmetric images of those with  $\eta_0 < 0$  shown in Fig. 3 which correspond to the solibores propagating downstream. It is important to note that the solution for  $\eta_0 = -1$  corresponds to the limit of an infinitesimally shallow bottom layer. As seen, the solibore shape in this limiting case is very similar to that of the gravity current found by Benjamin (1968). The difference is mostly at the bottom which is approached tangentially by the bore whereas the gravity current approaches it at the angle of  $\pi/3$  (von Kármán, 1940). This exact inviscid solution, which contains a singularity at the contact point where the velocity varies as  $\sim r^{-1/2}$  with the distance  $r$ , is outside the scope of the SW approximation.

## 5 Summary and discussion

In the present paper, we considered a special type of hydraulic jumps which, in the two-layer Boussinesq system bounded by a rigid lid, can conserve not only the mass and impulse, as usual, but also the circulation and energy. This is possible only at certain combinations of

the upstream and downstream states for which the speed of propagation becomes invariant with the free parameter specifying the contribution of each layer to the interfacial pressure distribution in the generalised SW momentum conservation law.

Jumps propagating into a quiescent fluid are fully conservative only if the interface upstream is located at the mid-height of the channel. The velocity of propagation of such jumps is independent of their height and equal to  $\dot{\xi} = 0.5$  in the dimensionless Froude number units. These fully conservative jumps have a special symmetry with the upstream shear being equal to the downstream interface height and vice versa:  $\vartheta_{\pm} = \eta_{\mp}$ . This symmetry ensures the automatic conservation of the impulse and energy as well as the continuity of both characteristic velocities across the jump. Namely, the positive and negative characteristics emanating on one side of the jump are parallel to the corresponding characteristics emanating on the other side.

Using this property we identified a broader class of fully conservative symmetric jumps which propagate in shear flows with the velocity  $\dot{\xi} = \pm \frac{1}{2}(1 + \eta_+ \eta_-)$ . The  $\pm$  sign here reflects the fact that, in the inviscid approximation, these jumps can theoretically propagate in either direction. In real fluids, which are viscous, physical considerations suggest that they have to propagate in the direction that increases the shear. For example, a jump leaving a viscous fluid right behind it at rest would be unphysical.

We also found that if the shear upstream and downstream is marginally hyperbolic with  $\vartheta_+ = \vartheta_- = \mp 1$ , another type of conservative jumps are possible. These jumps are in general asymmetric, have discontinuous characteristic velocities and propagate at the speed  $\dot{\xi} = \pm \frac{1}{2}(\eta_+ + \eta_-)$ . Because of the very specific shear values required for the existence of this type of jumps, they appear of little practical relevance.

It is important to note that the fully conservative jumps considered in this study satisfy four conditions but constrain only three out of five jump parameters. Namely, such jumps still have two degrees of freedom – the upstream and downstream interface heights. This is obviously due to the  $\eta \leftrightarrow \vartheta$  symmetry which is an exclusive feature of the Boussinesq approximation enabling the automatic conservation of two quantities.

Finally, the characteristics of fully conservative jumps were shown to be the same as those of the so-called solibores which appear as permanent-shape solutions in weakly non-hydrostatic approximation. An exact analytical solution for solibores was obtained.

Note that two such fully conservative jumps advancing into a quiescent fluid feature in the partial lock exchange flow when the lock is taller than the channel mid-height (Politis & Priede, 2022). These jumps represent the front of a gravity current propagating downstream along the bottom and a bore propagating upstream in the upper half of the channel. Analytical solution (39) can be seen in figure 4 to agree well with the two-dimensional DNS results of Khodkar *et al.* (2017) when the  $x$ -axis is scaled by a factor of  $\sqrt{2}$ . The agreement for the solibore is very good for both heights of the lock considered. The gravity current in turn can be seen to agree very well with the inviscid solution obtained by Benjamin (1968) which, as discussed above, slightly differs from the respective solibore solution in the vicinity of the contact point. It is interesting to note that both cases are equivalent in the SW approximation but treated somewhat differently in the conventional control volume approach. This, however, has no effect on the predicted speed propagation which is the same for gravity currents (Benjamin, 1968) and internal bores with a vanishingly shallow downstream bottom layer (Klemp *et al.*, 1997).

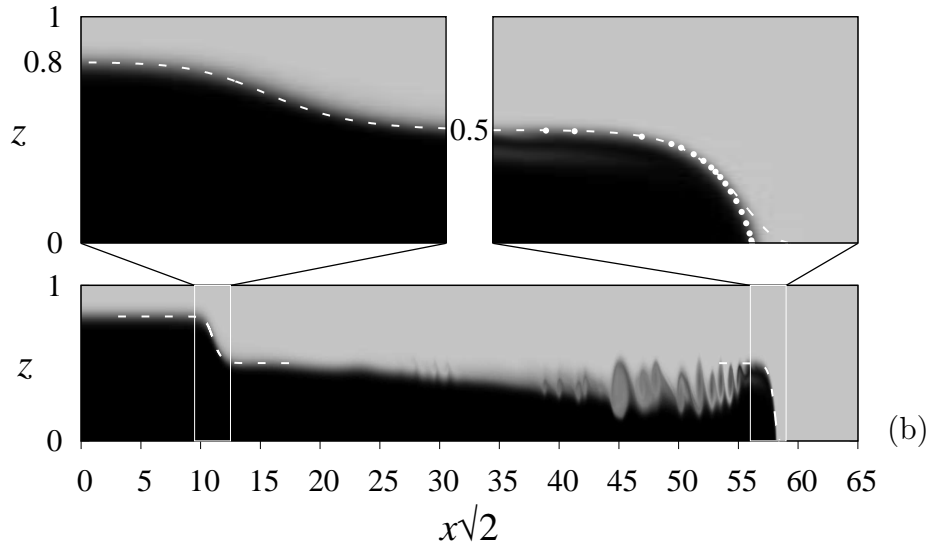
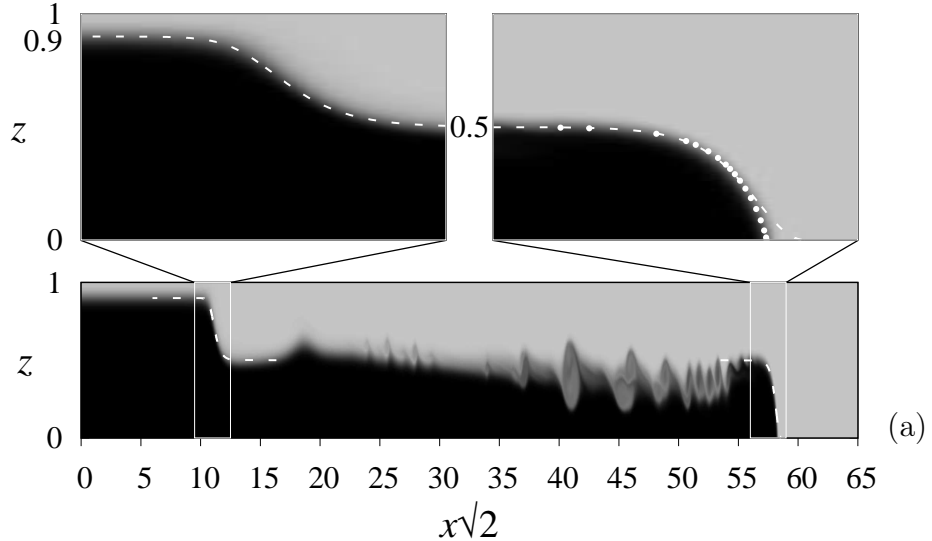


Figure 4: Comparison of the analytical solution (39) with the DNS results of Khodkar *et al.* (2017) for partial lock exchange flows with the lock height  $h_+ = 0.9$  (a) and  $h_+ = 0.8$  (b). The dashed lines show the analytical solution and the dots show the approximate solution for the energy conserving gravity current obtained by Benjamin (1968). The DNS results shown in the background are from figures 9(e,f) of Khodkar *et al.* (2017).

The finding that certain large-amplitude hydraulic jumps can be fully conservative while most are not such even in the inviscid approximation, points toward the wave dispersion as a primary mechanism behind the lossy nature of internal bores. Namely, it is the absence of dispersion in solibores that makes the corresponding jumps fully conservative while all other jumps are in general dispersive (Esler & Pearce, 2011). Such dispersive jumps may be amenable to Whitham's modulation theory (Whitham, 1965; El & Hoefer, 2016) which could resolve the non-uniqueness in their speed of propagation emerging in the hydrostatic SW approximation.

## References

BAINES, P. G. 1995 *Topographic effects in stratified flows*. Cambridge University Press.

BENJAMIN, T. B. 1968 Gravity currents and related phenomena. *J. Fluid Mech.* **31** (2), 209–248.

BENJAMIN, T. B. 1986 On the boussinesq model for two-dimensional wave motions in heterogeneous fluids. *J. Fluid Mech.* **165**, 445–474.

BORDEN, Z. & MEIBURG, E. 2013 Circulation-based models for Boussinesq internal bores. *J. Fluid Mech.* **726**, R1.

CAMASSA, R., CHEN, S., FALQUI, G., ORTENZI, G. & PEDRONI, M. 2012 An inertia 'paradox' for incompressible stratified euler fluids. *J Fluid Mech* **695**, 330–340.

CAVANIE, A. G. 1969 Sur la genese et la propagation d'ondes internes dans un milieu a deux couches. *Cahiers Océanographiques* **XXI** (9), 831–843.

CHOI, W. & CAMASSA, R. 1999 Fully nonlinear internal waves in a two-fluid system. *J. Fluid Mech.* **396**, 1–36.

CHRISTIE, D. R. & WHITE, R. 1992 The morning glory of the Gulf of Carpentaria. *Aust. Meteorol. Mag* **41**, 21–60.

CHUMAKOVA, L., MENZAQUE, F. E., MILEWSKI, P. A., ROSALES, R. R., TABAK, E. G. & TURNER, C. V. 2009 Stability properties and nonlinear mappings of two and three-layer stratified flows. *Stud. Appl. Math.* **122** (2), 123–137.

EL, G.A. & HOEFER, M.A. 2016 Dispersive shock waves and modulation theory. *Physica D* **333**, 11–65.

ESLER, J. G. & PEARCE, J. D. 2011 Dispersive dam-break and lock-exchange flows in a two-layer fluid. *J. Fluid Mech.* **667**, 555–585.

FYHN, E. H., LERVÅG, K. Y., ERVIK, Å. & WILHELMSEN, Ø. 2019 A consistent reduction of the two-layer shallow-water equations to an accurate one-layer spreading model. *Phys. Fluids* **31** (12), 122103.

GREEN, A. E. & NAGHDI, P. M. 1976 Directed fluid sheets. *Proc. R. Soc. Lond. A* **347** (1651), 447–473.

KHODKAR, M. A., NASR-AZADANI, M. M. & MEIBURG, E. 2017 Partial-depth lock-release flows. *Phys. Rev. Fluids* **2** (6), 064802.

KLEMP, J. B., ROTUNNO, R. & SKAMAROCK, W. C. 1997 On the propagation of internal bores. *J. Fluid Mech.* **331**, 81–106.

LISKA, R., MARGOLIN, L. & WENDROFF, B. 1995 Nonhydrostatic two-layer models of incompressible flow. *Computers Math. Applic.* **29** (9), 25–37.

LONG, R. R. 1956 Long waves in a two-fluid system. *J. Meteor.* **13** (1), 70–74.

MILEWSKI, P., TABAK, E., TURNER, C., ROSALES, R. & MENZAQUE, F. 2004 Nonlinear stability of two-layer flows. *Comm. Math. Sci.* **2** (3), 427–442.

MILEWSKI, P. A. & TABAK, E. G. 2015 Conservation law modelling of entrainment in layered hydrostatic flows. *J. Fluid Mech.* **772**, 272–294.

OVSYANNIKOV, L. V. 1979 Two-layer "shallow water" model. *J. Appl. Mech. Tech. Phys.* **20** (2), 127–135.

POLITIS, G. & PRIEDE, J. 2022 Lock-exchange problem for Boussinesq fluids revisited: Exact shallow-water solution. *Phys. Fluids* **34**, 106602.

PRIEDE, J. 2022 Self-contained two-layer shallow water theory of strong internal bores. *Stud. Appl. Math.* pp. 1–24, doi:10.1111/sapm.12546.

RAYLEIGH, LORD 1914 On the theory of long waves and bores. *Proc. Roy. Soc. Lond. A* **90** (619), 324–328.

SANDSTROM, H. & QUON, C. 1993 On time-dependent, two-layer flow over topography. i. hydrostatic approximation. *Fluid Dyn. Res.* **11** (3), 119.

SCOTTI, A. & PINEDA, J. 2004 Observation of very large and steep internal waves of elevation near the massachusetts coast. *Geophys. Res. Lett.* **31** (22).

SIMPSON, J. E. 1999 *Gravity currents: In the environment and the laboratory*, 2nd edn. Cambridge University Press.

VON KÁRMÁN, T. 1940 The engineer grapples with nonlinear problems. *Bull. M. Math. Soc.* **46** (8), 615–683.

WHITHAM, G. B. 1965 Non-linear dispersive waves. *Proc. R. Soc. Lond. A* **283** (1393), 238–261.

WHITHAM, G. B. 1974 *Linear and Nonlinear Waves*. Wiley.

WOOD, I. R. F. & SIMPSON, J. E. 1984 Jumps in layered miscible fluids. *J. Fluid Mech.* **140**, 329–342.